J Physiol 586.17 (2008) pp 4209–4223

Nitric oxide–cGMP–protein kinase G pathway negatively regulates vascular transient receptor potential channel TRPC6

Shinichi Takahashi[1], Hai Lin[1], Naomi Geshi[1,4], Yasuo Mori[2], Yasuhiro Kawarabayashi[1], Noboru Takami[3], Masayuki X. Mori[1], Akira Honda[1] and Ryuji Inoue[1]

[1] *Department of Physiology and* [3] *Radioisotope Laboratory, Graduate School of Medical Sciences, Fukuoka University, Fukuoka 814-0180, Japan*
[2] *Laboratory of Molecular Biology, Department of Synthetic Chemistry and Biological Chemistry, Graduate School of Engineering, Kyoto University, Kyoto 615-8510, Japan*
[4] *Department of Plant Biology and Biotechnology, Faculty of Life Sciences, University of Copenhagen, DK-1871 Frederiksberg C, Denmark*

We investigated the inhibitory role of the nitric oxide (NO)–cGMP–protein kinase G (PKG) pathway on receptor-activated TRPC6 channels in both a heterologous expression system (HEK293 cells) and A7r5 vascular myocytes. Cationic currents due to TRPC6 expression were strongly suppressed (by ∼70%) by a NO donor SNAP (100 μM) whether it was applied prior to muscarinic receptor stimulation with carbachol (CCh; 100 μM) or after G-protein activation with intracellular perfusion of GTPγS (100 μM). A similar extent of suppression was also observed with a membrane-permeable analogue of cGMP, 8Br-cGMP (100 μM). The inhibitory effects of SNAP and 8Br-cGMP on TRPC6 channel currents were strongly attenuated by the presence of inhibitors for guanylyl cyclase and PKG such as ODQ, KT5823 and DT3. Alanine substitution for the PKG phosphorylation candidate site at T69 but not at other sites (T14A, S28A, T193A, S321A) of TRPC6 similarly attenuated the inhibitory effects of SNAP and 8Br-cGMP. SNAP also significantly reduced single TRPC6 channel activity recorded in the inside-out configuration in a PKG-dependent manner. SNAP-induced PKG activation stimulated the incorporation of ^{32}P into wild-type and S321A-mutant TRPC6 proteins immunoprecipitated by TRPC6-specific antibody, but this was greatly attenuated in the T69A mutant. SNAP or 8Br-cGMP strongly suppressed TRPC6-like cation currents and membrane depolarization evoked by Arg^8-vasopressin in A7r5 myocytes. These results strongly suggest that TRPC6 channels can be negatively regulated by the NO–cGMP–PKG pathway, probably via T69 phosphorylation of the N-terminal. This mechanism may be physiologically important in vascular tissues where NO is constantly released from vascular endothelial cells or nitrergic nerves.

(Received 29 April 2008; accepted after revision 8 July 2008; first published online 10 July 2008)
Corresponding author R. Inoue: Department of Physiology, Graduate School of Medical Sciences, Fukuoka University, Fukuoka 814 0180, Japan. Email: inouery@fukuoka-u.ac.jp

In the cardiovascular system, nitric oxide (NO) plays an important regulatory role controlling haemodynamics and vascular remodelling. NO stimulates soluble guanylyl cyclases (GCs) to generate the second messenger cyclic GMP (cGMP), which in turn activates cGMP-dependent protein kinase G (PKG) and phosphodiesterases (Lincoln *et al.* 2001; Feil *et al.* 2003; Hofmann *et al.* 2006). One of the principal consequences of PKG activation in blood vessels (or vascular smooth muscle cells; VSMCs) is vasorelaxation, which is mediated by phosphorylation of proteins that regulate the intracellular Ca^{2+} levels as well as the sensitivity of the contractile machinery. As for the reduction in $[Ca^{2+}]_i$ caused by PKG, several distinct mechanisms have been proposed (Lincoln *et al.* 2001; Feil *et al.* 2003). It has been reported that the increased activity of the BK_{Ca} ($K_{Ca}1.1$) channel following PKG activation produces membrane hyperpolarization thereby decreasing the rate of Ca^{2+} entry into VSMCs through voltage-dependent Ca^{2+} channels (VDCCs). Phosphorylation of the inositol 1,4,5-trisphosphate receptor (IP_3R)-associated protein IRAG (IP_3R-associated PKG substrate) is thought to inhibit agonist-induced Ca^{2+} release from internal stores. The possibility has also been suggested that phosphorylation of phospholamban

S. Takahashi and H. Lin contributed equally to this work.
This paper has online supplemental material.

DOI: 10.1113/jphysiol.2008.156083

by PKG may increase the activity of sarcoplasmic Ca^{2+}-ATPase, facilitating the active transport of Ca^{2+} into internal stores and thereby decreasing $[Ca^{2+}]_i$. In addition to these, in many different types of blood vessels, activation of PKG has been found to inhibit vasoconstrictor-induced Ca^{2+} influx through plasmalemmal pathways other than VDCCs (Karaki *et al.* 1997). There has, however, been considerable paucity of information about the molecular entity of such Ca^{2+} influx pathways, and accordingly, it remains unclear how phosphorylation via PKG activation reduces the rate of Ca^{2+} influx.

Recent studies on the transient receptor potential (TRP) proteins have established them as components of large non-voltage-gated Ca^{2+} channels, the members of which family are activated in response to stimulation of phospholipase C (PLC)-linked receptors, through, for instance, heat, acid, hypo-osmolarity, oxidative stress and several artificial somatosensory stimulants (Ramsey *et al.* 2006). Of this unique family, TRPC6, which is widely distributed in the vasculature and heart, has been implicated in the pathophysiology of the cardiovascular system (Inoue *et al.* 2006; Dietrich *et al.* 2007). There is good evidence to suggest that vasoconstrictive neurotransmitters and hormones (noradrenaline, angiotensin II, vasopressin, etc.) activate the TRPC6 channel to increase the rate of transmembrane Ca^{2+} entry contributing to vascular tone generation and smooth muscle proliferation (Inoue *et al.* 2001; Soboloff *et al.* 2005; Hill *et al.* 2006; Saleh *et al.* 2006), and the dysregulation of this Ca^{2+} entry may underlie pulmonary and essential hypertensions and cardiomyopathy (McKinsey & Olson, 2005; Kuwahara *et al.* 2006; Firth *et al.* 2007; Inoue *et al.* 2008). It is well established that diacylglycerol (DAG) and related phosphoinositides/metabolites (PIP_2, PIP_3, IP_3) fulfil a central role in the activation/inactivation processes of at least three TRPC members: TRPC3, TRPC6 and TRPC7 (Kwon *et al.* 2007; Lemonnier *et al.* 2007). These channels also appear to be effectively regulated by protein kinase-mediated phosphorylation (Yao *et al.* 2005). For example, in the early phase of receptor stimulation, phosphorylation of TRPC6 by Ca^{2+}–calmodulin-dependent kinase II (CaMKII) increases the availability of the channel thereby accelerating its activation (Shi *et al.* 2004). Activation of TRPC3 and TRPC6 channels is positively regulated by tyrosine phosphorylation following stimulation of GPCRs as well as growth hormone receptors (Hisatsune *et al.* 2004; Vazquez *et al.* 2004). In contrast, when the receptor stimulation is prolonged, negative regulation of the channels via PKC-mediated phosphorylation becomes dominant, leading to their inactivation (Shi *et al.* 2004; Trebak *et al.* 2005). Furthermore, store-operated or DAG-induced Ca^{2+} influx associated with overexpression of TRPC3 protein has been shown to be diminished by pretreatment with agents increasing intracellular cGMP levels, where PKG-mediated phosphorylation plays a pivotal role (Kwan *et al.* 2004). Mutagenesis scanning together with phosphorylation assay has revealed that the sites responsible for this inhibition may reside on the threonine 11 and serine 263 of the N-terminus of the TRPC3 channel; homologous sites are also present in TRPC6 and TRPC7 channels (Kwan *et al.* 2004). Interestingly, the phosphorylation of the latter site (Ser263) also seems to involve an as-yet unclarified, indirect activation of PKG via PKC, the same mechanism probably operating in native vascular endothelial cells (VECs) (Kwan *et al.* 2006).

Despite such supportive evidence, however, direct demonstration of the negative regulation of TRPC3 channels by PKG using ionic current recording is still lacking, and there is no functional/biochemical evidence available for PKG-mediated regulation of TRPC6 or TRPC7 channels. To resolve these uncertainties, we investigated the effects of PKG activation on the TRPC6 channel and its native counterpart in A7r5 cells, which are established rat embryonic aortic myocytes, and looked for the molecular mechanisms involved using patch clamp and phosphorylation assay. As a result, we have found that, regardless of the system employed (i.e. heterologous expression or native), the activity of TRPC6 channels is markedly suppressed by PKG activation, and that phosphorylation on Thr69 but not on Ser321 of TRPC6, the sites homologous to Thr11 and Ser263 of TRPC3, respectively, is essential for this. A preliminary account of this work has been communicated to the 84th annual meeting of the Japanese Physiological Society (Takahashi *et al.* 2007).

Methods

Materials

The full length of TRPC6 DNA was cloned from the mouse brain cDNA library. Single amino acid mutations were introduced by PCR techniques using the QuikChange Site-directed Mutagenesis Kit (Stratagene, San Diego, USA) according to the manufacturer's instructions. Both wild-type and mutant TRPC6 DNAs were subcloned into the pCI-neo expression vector and their authenticity and accuracy were verified by direct sequencing with a 3100 genetic analyser (Applied Biosystems, Hitachi).

Polyclonal anti-TRPC6 antibody was purchased from Alomone (No. ACC017).

Cell culture and transfection

The human embryonic cell line HEK293 and the rat embryonic aortic cell line A7r5 were purchased from ATCC (Manassas, VA, USA) and maintained in

Dulbecco's modified culture medium (DMEM) under 5% CO_2 with passage every 3–4 day. DMEM was supplemented with 10% fetal bovine serum, and a mixture of antibiotics (100 units ml^{-1} penicillin–streptomycin; Gibco).

TRPC6 DNA was transfected together with pCI-neo-πH3-CD8 (cDNA of the T-cell antigen CD8) at a ratio of 5–10 : 1, to HEK cells which had reached 50–80% confluency. To enhance the transfection efficiency, a transfection reagent SuperFect· (Qiagen, Germany) was used. Functional evaluation was made 48–72 h after transfection, when the expression of TRPC6 proteins reached their peak. To select cells successfully expressing TRPC6 proteins, polystyrene beads conjugated with anti-CD8 antibody (Dynabeads M-450 CD8, Dynal Biotech) were used as the expression marker, as performed previously (Shi *et al.* 2004).

To knockdown TRPC6 expression, 40–50 pmol ml^{-1} stealth–siRNA duplex (from 5′ to 3′): AAACCACCGUUGCAUAAAGACC and GGUCUUUAUGCAAUCGCGGUGGUUU, were transfected to 30–50% confluent A7r5 myocytes with the aid of 2.5 μl ml^{-1} lipofectamine 2000 according to the manufacturer's instruction (Invitrogen, USA). After 60–72 h, almost complete elimination of TRPC6 protein expression was confirmed by immunoblotting (see, e.g., the inset in Fig. 8*A*).

Electrophysiology and data analysis

The details of patch clamp recordings and data analyses were essentially the same as previously described (Shi *et al.* 2007). In brief, patch electrodes with a resistance of 2.5–4 MΩ (when filled with internal solution) were made from 1.5 mm boroscilicate glass capillaries using an automated electrode puller (Sutter Instruments) and heat polished. Voltage generation and current signal acquisition used a high-impedance low-noise patch clamp amplifier (EPC9; HEKA Electronics, Germany) in conjunction with an A/D, D/A-converter (Digidata 1200; Axon Instruments). Sampled data were low-pass filtered at 1 kHz, digitized at 5 kHz and analysed using Clampfit v. 9.2 (Axon Instruments). Longer time-frame recordings (e.g. whole-cell current traces in Fig. 1) were performed with PowerLab/400 (ADInstruments, Australia; sampling rate, 100 Hz), and data evaluation was made by using the accessory software Chart v3.6. The magnitude of recorded noisy currents was defined as their 5–10 s averages over the time period of concern.

For current clamp recording, K^+ internal solution (below) was used. Artificial leak currents occurring after whole-cell conditions were established seemed to seriously affect the value and stability of the membrane potential. Thus, cells showing more than −10 pA at −50 mV were not included in the evaluation.

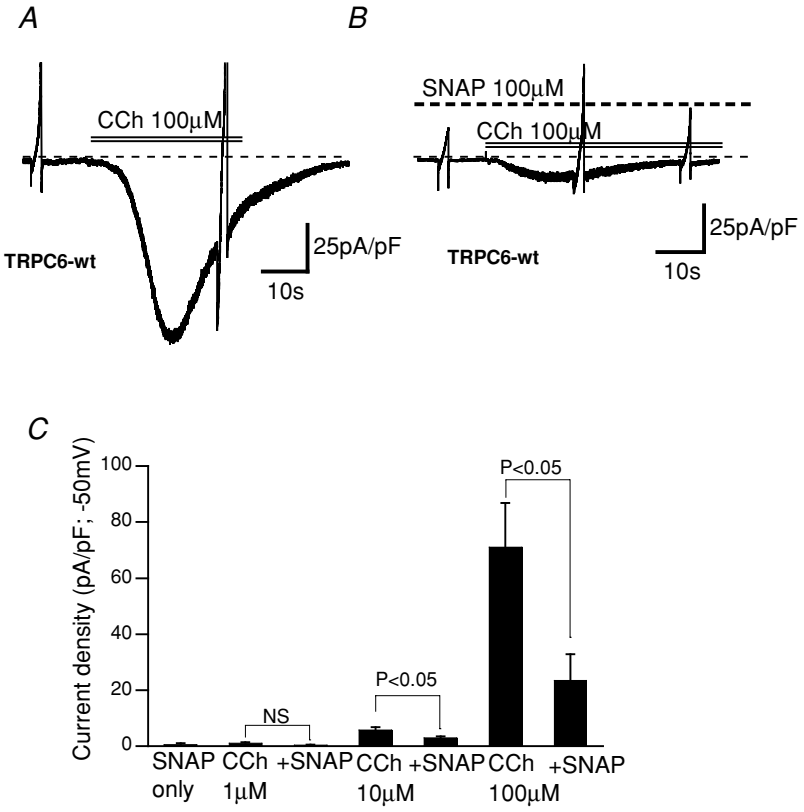

Figure 1. NO donor SNAP inhibits receptor-activated TRPC6 currents (I_{TRPC6})
A and *B*, actual current traces of inward cation currents activated by muscarinic receptor stimulation (CCh; 100 μM) in the absence (*A*) and presence (*B*) of 100 μM SNAP. Murine TRPC6-expressing HEK293 cells were voltage clamped at −50 mV. Bath, normal PSS; pipette, caesium aspartate internal solution. SNAP was added into the bath 5–10 min before application of CCh. *C*, summary of the density of inward currents induced by SNAP (1 mM) alone, CCh (1, 10, 100 μM) alone, and pretreatment with SNAP (100 μM) for 5–10 min and subsequent application of CCh (1, 10, 100 μM). $n = 6$–8.

For single channel recordings in the inside-out (I/O) configuration, electrodes having a resistance of 3–4 MΩ (with the pipette solution described below) were used. Sampled data were low-pass filtered at 1 kHz and stored on a computer hard disc after digitization at 5 kHz. Single channel analysis was made using the software Clampfit v. 9.2 (Axon Instruments). The mean single channel current (NP_oi) was calculated for each experiment in the absence and presence of drugs by averaging the current amplitude over 5 s with respect to the baseline as performed previously (Shi *et al.* 2007).

Drugs were rapidly applied onto cells or excised patch membranes by using a fast solution change device called 'Y-tube' as previously described (Shi *et al.* 2004). All experiments were performed at room temperature (22–26°C).

Immuunocytochemistry

Anti-TRPC6 rabbit antibody targeting the C-terminal sequence 'RRNESQDYLLMDELG' (TRPC6: 24–38) was purchased from Alomone. HEK293 cells overexpressing wild-type TRPC6 protein were plated on round coverslips and then fixed with 4% paraformaldehyde for 15 min and permeabilized with 0.2% Triton–PBS for 15 min at room temperature. After rinsing in PBS several times, the cells were pre-incubated for 1 h with 10% normal goat serum (NGS; Wako, Japan), and incubated successively with 1 : 200 diluted TRPC6 antibody overnight at 4°C, and with Alexa 488-labelled anti-rabbit goat antiserum (Invitrogen, USA) for 1 h after washing with PBS. The coverslips were sealed with PermaFluor Aqueous (Immunon Shandon) to prevent evaporation. Immunofluorescence was observed under a confocal laser scanning microscope (FV1000, Olympus, Japan) equipped with an argon–krypton laser source. A single wavelength of 488 nm was used for excitation, and the emitted fluorescence at 505 nm was collected through an oil-immersion objective lens with 40× magnification. The spatial profile of immunofluorescence was assessed by the 'plot profile' function of free NIH software 'ImageJ' v. 1.33 μ.

Western blotting

After rising with PBS, the total lysate of A7r5 myocyes (about 10^6 cells) was prepared in sample buffer. The protein concentration of the sample was determined using the BCA protein assay kit (Pierce). 2-Mercaptoethanol (5% v/v) and bromophenol blue (1% w/v) were added to the sample, and proteins were separated by 10% (w/v) SDS-PAGE electrophoretically and electroblotted to a polyvinylidene diflouride (PVDF) membrane. The membrane was blocked with 5% (w/v) skimmed milk dissolved in Tween–PBS, and then incubated with the anti-TRPC6 antibody (Alomone; see above) (at 1 : 200 dilution) overnight. TRPC6 protein (∼120 kDa) was visualized by chemiluminescence, incubating the PVDF membrane with the secondary antibody linked to horseradish peroxidase, and analysed densitometrically.

In vitro PKG phosphorylation assay

Wild-type and mutant TRPC6 proteins overexpressed in HEK293 cells were extracted, and aliquots containing the same amounts were subjected to immunoprecipitation with anti-rabbit TRPC6 antibody (overnight at 4°C), and collected on protein A Sepharose beads. We confirmed that the expression level of TRPC6 proteins relative to total protein were comparable between wild and mutant proteins by Western blotting. After rinsing with the lysis buffer, immunoprecipitates were incubated in phosphorylation buffer at 37°C for 5 min, to which active PKG Iα (40 ng per reaction) and 0.125 μCi μl^{-1} [γ-^{32}P]ATP (1 Ci = 37 GBq) was successively added. The phosphorylation reaction was performed at 37°C for 5 min and stopped by transferring the reaction tube onto ice and then incubating it with 30 μl reaction laemmli buffer at 95°C for 5 min. The phosphorylation products yielded were subjected to SDS-PAGE, followed by autoradiography. The composition of lysis buffer was 1% Nonidet, 150 mM NaCl, 20 mM Tris-HCl (pH 8) supplemented with protein inhibitor cocktail (Sigma); the phosphorylation buffer was (mM): Tris-HCl 30, $MgSO_4$ 1, EDTA 1, ATP 0.04 and cGMP 0.01, and 1 μM KT5720 was added to prevent the cross-activation of PKA. The PKG inhibitor KT5823 was also added to the buffer as needed. To quantify the amount of ^{32}P incorporation, ImageJ v. 1.33 μ was used.

Solutions and chemicals

The pipette solution for whole-cell recording contained (mM): 120 CsOH, 120 aspartate, 20 CsCl, 2 $MgCl_2$, 10 BAPTA/4 $CaCl_2$ (or 5 EGTA/1.5 $CaCl_2$), 10 Hepes, 2 ATP, 0.1 GTP, 10 glucose (adjusted to pH 7.2 with Tris base); the pipette solution for current clamp recording contained (mM): 140 KCl, 2 $MgCl_2$, 1 EGTA, 10 Hepes, 2 ATP, 0.1 GTP, 10 glucose (adjusted to pH 7.2 with Tris base). The external solution contained (mM): 140 NaCl, 5 KCl, 1 $CaCl_2$, 1.2 $MgCl_2$, 10 Hepes, 10 glucose (pH 7.4, adjusted with Tris base).

The pipette solution for I/O recording contained (mM): 140 NaCl, 5 tetraethylammonium-Cl, 0.1 DIDS, 1.2 $MgCl_2$, 1 $CaCl_2$, 10 Hepes, 10 glucose, 0.1 carbacol (CCh) (pH 7.4, adjusted with Tris base). Bathing solution for I/O recording contained (mM): 120 CsOH, 120 aspartate, 20 CsCl, 2 $MgSO_4$, 2 EGTA, 0.4 Ca, 10 Hepes, 2 ATP, 0.1 GTP (pH 7.2, adjusted with Tris base).

CCh and GTPγS, were purchased from Sigma-Aldrich (USA), and AVP ([Arg^8]-vasopressin), SNAP (*S*-nitroso-*N*-acetylpenicillamine), NOR-3 ((+/−)-(E)-ethyl-2-[(E)-hydroxyimino]-5-nitro-3-hexeneamide), 8Br-cGMP (8Br-cGMP), ODQ (1H-[1,2,4]oxadiazolo [4,3-a]quinoxalin-1-one), KT5823, DT3 (membrane-permeable protein kinase G Iα inhibitory peptide: RQIKIWFQNRRMKWKKLRKKKKKH) from Calbiochem-Merck (USA).

Stock solutions for drugs were made by dissolving their powders in DMSO at more than 1000-fold higher concentrations than needed for experimental use, so that the highest concentration of DMSO used did not exceed 0.1%, which did not affect the magnitude or kinetics of TRPC6 currents significantly.

Statistics

All data are expressed as means ± S.E.M. Paired and unpaired Student's *t* test was used to evaluate statistical significance with a criterion of $P < 0.05$. For multiple comparison, statistical significance was evaluated by ANOVA followed by Bonferroni's *t* test.

Results

NO donors inhibit CCh- or GTPγS-induced TRPC6 currents

In the first step of this study, we examined the effects of a NO donor, SNAP, on basal currents in TRPC6-expressing HEK293 cells in the absence of receptor stimulation, since NO donors have been shown to directly activate a few members of the TRPC subfamily via *S*-nitrosylation (Yoshida *et al.* 2006). However, as demonstrated and summarized in Fig. 1*B* and *C*, respectively, bath application of SNAP up to 1 mM failed to produce discernible currents (−0.5 ± 0.5 pA at −50 mV with 1 mM SNAP, $n = 7$). The same result was obtained with another NO donor, NOR-3 (300 μM; data not shown). This observation confirms the previous finding that NO donors did not induce detectable changes in $[Ca^{2+}]_i$ in HEK cells overexpressing TRPC6 protein which lacks the target cysteines responsible for *S*-nitrosylation (Yoshida *et al.* 2006).

In the continued presence of SNAP (100 μM) applied 3–5 min beforehand, however, the magnitude of inward currents subsequently induced by CCh (100 μM; I_{TRPC6}) in TRPC6 expressing HEK cells was greatly reduced (∼70%), without significant change in the time course of activation (time to peak activation; 19.6 ± 4.4 s *versus* 24.1 ± 6.3 s in the absence and presence of 100 μM SNAP, respectively, $n = 7$; Fig. 1*A*–*C*). This inhibition also appeared to occur independently of the extent of receptor stimulation as can be seen with lower concentrations of CCh (1 and 10 μM), which did not affect the extent of inhibition (Fig. 1*C*)

A similar extent of inhibition was also observed when SNAP (Fig. 2*A* and *B*) or a structurally different NO donor NOR-3 (filled circle in Fig. 2*B*) was applied after I_{TRPC6} had already been activated by intracellular perfusion of GTPγS (100 μM). The inhibition occurred dose dependently (open circles in Fig. 2*B*) and its time course was so rapid it was almost complete within a minute (time from the onset of 100 μM SNAP application to 50% I_{TRPC6} inhibition; 37.3 ± 7.1 s, $n = 10$). The degree of this inhibition was independent of voltage as can be seen by the almost uniform suppression of the I_{TRPC6} current–voltage relationship over a wide range of membrane potentials (Fig. 2*C* and *D*), indicating no obvious voltage dependence on the inhibitory actions of SNAP on I_{TRPC6}.

The SNAP-induced inhibition of the TRPC6 channel could also be observed as slowing of the divalent cation entry in response to receptor stimulation. Although interpretation is limited because of the possible contribution of store depletion, the rate of CCh-enhanced Ba^{2+} influx in TRPC6-expressing cells was greatly reduced after treatment with 100 μM SNAP (online Supplemental Fig. 1).

The inhibitory effect of NO is mediated by the cGMP–PKG pathway

In general, NO is thought to stimulate soluble GC to increase the intracellular cGMP level, thereby activating PKG (Lincoln *et al.* 2001; Feil *et al.* 2003). We therefore tested whether this classic signalling pathway is indeed involved in the inhibitory effect of SNAP on I_{TRPC6} by using both a mimetic and inhibitors of cGMP and PKG. As summarized in Fig. 3*C* and *E* (for actual traces, see Fig. 1*A*, *B* and *D*), activation of PKG by a membrane-permeable analogue of cGMP, 8Br-cGMP (8Br-cGMP; 100 μM) resulted in a similar extent of I_{TRPC6} inhibition regardless of whether CCh or GTPγS was used as the activator. Conversely, the inhibitors for GC and PKG (isoform Iα), ODQ (100 μM), KT5823 (1 μM) and DT3 (1 μM), respectively, abolished the inhibition of I_{TRPC6} by SNAP or 8Br-cGMP almost completely (Fig. 3*C* and *E*). In addition, selective inhibition of PKG with DT3 (1 μM) did not itself enhance the magnitude (or density) of I_{TRPC6} induced by CCh (100 μM) (Fig. 3*E*). Since this concentration of CCh was high enough to stimulate the muscarinic receptor thereby activating PKC, at least in physiological conditions, these results show that indirect stimulation of PKG via PKC activation does not contribute significantly to the inhibition of I_{TRPC6} (cf. Kwan *et al.* 2006).

The inhibitory effects of SNAP on macroscopic I_{TRPC6} could also be seen at the single channel level. As displayed and summarized in Fig. 4*A* and *B*, respectively, single CCh-induced cationic channel activity recorded from I/O membranes excised from TRPC6-expressing cells was

inhibited by addition of SNAP (100 μM), which was then reversed by administration of the PKG inhibitory peptide DT3 (1 μM).

The above results together suggest that elevation in intracellular cGMP and subsequent activation of PKG is intimately associated with the SNAP-induced inhibition of receptor-induced TRPC6 channel activity.

The amino acid residue responsible for SNAP-induced inhibition

The involvement of the cGMP–PKG pathway in SNAP- or 8Br-cGMP-induced inhibition suggests that the activity of TRPC6 channel protein may be directly regulated by its phosphorylation by PKG. To investigate this possibility, we searched for the consensus motif of PKG phosphorylation '$(R/K)_{2-3}$-X-(S/T)' over the whole amino acid sequence of the murine TRPC6 protein. As illustrated in Fig. 5*A*, five serine or threonine residues satisfying this criterion (T14A, S28A, T69A, T193A or S321A) were found only on the N-terminal region of mouse TRPC6 protein.

HEK cells expressing TRPC6 mutants carrying the alanine substitution for these serine/threonine residues all generated comparable magnitudes of inward cationic currents upon intracellular perfusion of GTPγS (100 μM) (an actual trace for T69A is displayed in Fig. 5*B*). Bath-application of SNAP (100 μM) produced a similar extent of inhibition of these currents, but as the sole

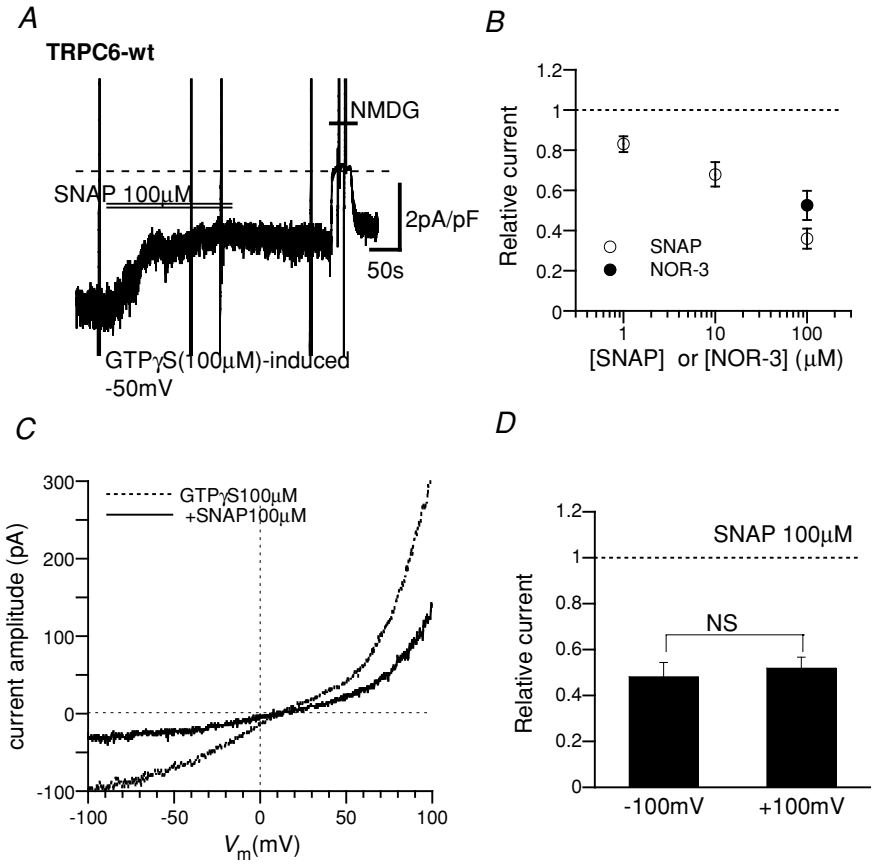

Figure 2. Inhibitory effects of SNAP and NOR-3 on GTPγS-induced I_{TRPC6}
A, representative trace for GTPγS-induced I_{TRPC6} at −50 mV. SNAP (100 μM), added at the bar, rapidly reduced the amplitude of I_{TRPC6}. At the end of the trace, external Na^+ was quickly replaced with a large impermeant cation *N*-methyl,D-glucamine (NMDG), which reversibly abolished the inward current. Experimental conditions were the same as in Fig. 1 except that GTPγS (100 μM) was added to the internal solution. *B*, SNAP concentration–I_{TRPC6} inhibition curve (○) and fractional inhibition of I_{TRPC6} by NOR-3 (100 μM; ●). Plotted data represent the relative amplitude of I_{TRPC6} 3 min after addition of SNAP or NOR-3 which is normalized to that just before the addition of drugs. $n = 4$–11. *C*, representative current–voltage relationships (*I–V* curves) of GTPγS-induced I_{TRPC6} before (dotted curve) and about 3 min after (continous curve) application of 100 μM SNAP. Slow rising voltages (−100 to +100 mV, 2 s) were applied to construct the *I–V* curves. *D*, the degree of SNAP-induced I_{TRPC6} inhibition at −100 and 100 mV. The relative current amplitude, which is calculated as the ratio of I_{TRPC6} amplitudes after to before application of 100 μM SNAP, was obtained from *I–V* curves such as shown in *C*. $n = 7$.

exception, the T69A mutant was almost unresponsive to SNAP as well as to 8Br-cGMP (Fig. 5*C*). Consistent with this observation, in the T69A mutant, SNAP did not significantly affect the magnitude of cation currents evoked by receptor stimulation with CCh (100 μM) (Fig. 5*D* and *E*).

These results strongly support the view that the phosphorylated status of T69 is crucial for negative

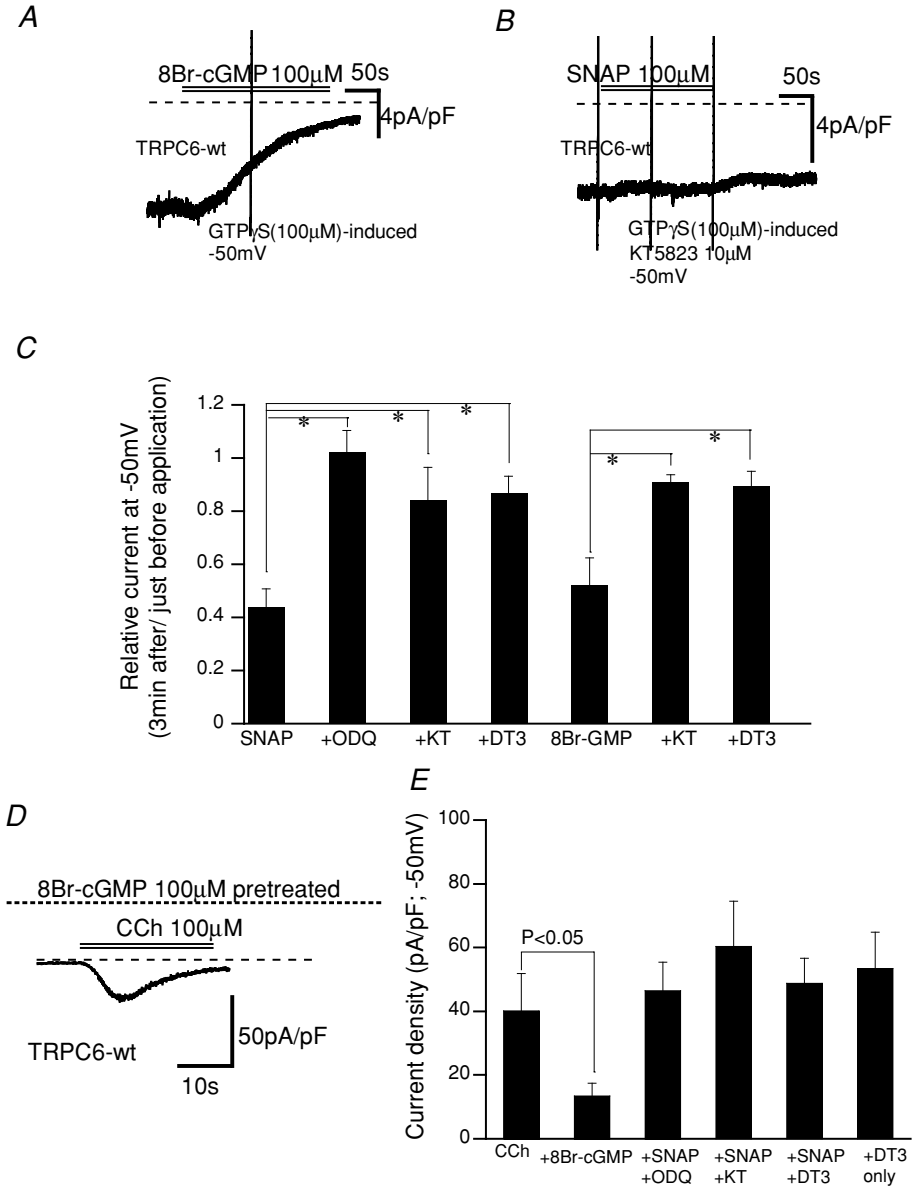

Figure 3. Effects of activators and inhibitors for the cGMP–PKG pathway on I_{TRPC6}
The experimental conditions were the same as in Figs 1 and 2. *A* and *B*, actual traces for GTPγS-induced I_{TRPC6} with (right) and without (left) addition of KT5823 (1 μM) in the pipette. *C*, summary of the effects of the cGMP–PKG pathway activators/inhibitors on GTPγS-induced I_{TRPC6}. From left to right; SNAP (100 μM): SNAP + ODQ (10 μM): SNAP + KT5823 (1 μM): SNAP + DT3 (1 μM): 8Br-cGMP (100 μM): 8Br-cGMP + KT5823 (1 μM): 8Br-cGMP + DT3 (1 μM). $n = 4$–7. $^*P < 0.05$. SNAP and 8Br-cGMP were applied to the bath, and other drugs were included in the patch pipette. Definition of relative current is the same as in Fig. 2. *D*, actual trace for CCh (100 μM)-induced I_{TRPC6} after 100 μM 8Br-cGMP treatment (5 min). *E*, summary of the effects of the cGMP–PKG pathway activators/inhibitors on CCh-induced I_{TRPC6}. Columns indicate the peak amplitude of CCh-induced I_{TRPC6} under each experimental condition, which is normalized by the cell capacitance. From left to right: control (CCh, 100 μM): 8Br-cGMP (100 μM; pretreated for 5–10 min): SNAP (100 μM; pretreated for 5–10 min) + ODQ (10 μM): SNAP + KT5823 (1 μM): SNAP + DT3 (1 μM): DT3 (1 μM) alone. ODQ, KT5823 and DT3 were included in the patch pipette. $n = 4$–10.

regulation of TRPC6 channel by the NO–cGMP–PKG pathway.

PKG phosphorylation is reduced in T69A mutant

To confirm the above functional data more directly, we next evaluated the *in vitro* phosphorylation by PKG of wild-type and mutant TRPC6 proteins by using the radioactive phosphorus (^{32}P) incorporation assay. As demonstrated in Fig. 6, the radioactivity of bands which represent the ^{32}P-phosphorylation of TRPC6 protein by PKG was significantly decreased by the presence of KT5823 for both wild-type and S321A mutant proteins. In contrast, this change was only modest in the T69A mutant. Quantification of the radioactivity clearly shows that the level of ^{32}P incorporation into T69A mutant proteins induced by PKG activation is significantly lower than that of wild-type or the S321A TRPC6 mutant which carries the alanine substitution for the 321st serine residue corresponding to another PKG phosphorylation site (S263) in human TRPC3 (Kwan *et al.* 2004). Residual PKG phosphorylation in the T69A mutant can be interpreted to indicate that other amino acid residues would be phosphorylated by PKG *in vitro*. However, the great reduction in PKG phosphorylation observed in the T69A mutant provides further support for the inhibitory role of PKG phosphorylation of T69 on TRPC6 channel activity.

Cellular localization of TRPC6 protein was not affected by activation of PKG

The overall activity of ion channels is often regulated by their membrane trafficking (Lippincott-Schwartz *et al.* 2000; Ma & Jan, 2002). We therefore questioned whether inhibition of TRPC6 channel activity by PKG phosphorylation may result from facilitated endocytosis of the channel protein, by comparing the cellular localization of TRPC6-sepcific immunoreactivity before and after treatment with SNAP. As demonstrated and summarized in Fig. 7, the cell membrane localized profile of TRPC6 immunofluorescence was not significantly altered by treatment with SNAP (100 μM). These results are compatible with the idea that altered gating rather than decreased cell surface expression may be responsible for SNAP-induced TRPC6 channel inhibition.

NO–cGMP–PKG pathway negatively regulates native TRPC-like current in A7r5 cells

Finally, to confirm the relevance of the results obtained for the expressed TRPC6 channel to the native system, we tested the possible role of the NO–cGMP–PKG signalling pathway in A7r5 myocytes, a widely used VSMC model. Activation of cationic currents by bath-application of Arg^8-vasopressin (AVP) or intracellular perfusion of GTPγS (Fig. 8*A* and *B*) was markedly attenuated in A7r5 cells in which TRPC6 protein expression had been eliminated through specific siRNA knockdown (inset in Fig. 8*A*). Similar findings have been reported by Soboloff *et al.* (2005). Importantly, application of SNAP or 8Br-cGMP caused a marked suppression of the cationic currents activated by intracellular GTPγS perfusion (Fig. 8*C* and *D*) and also reduced the rate of Ba^{2+} influx evoked by AVP (Supplemental Fig. 2), and the inhibitory effect of SNAP on GTPγS-induced cation currents was greatly reduced by inclusion of DT3 in the patch pipette. Consistent with these observations, the membrane depolarization induced by AVP (0.1 μM), which was almost completely abolished by substitution of Na^+ with an impermeant cation *N*-methyl, D-glucamine (NMDG), was significantly retarded and attenuated by pre-treatment with SNAP (100 μM) (the level of

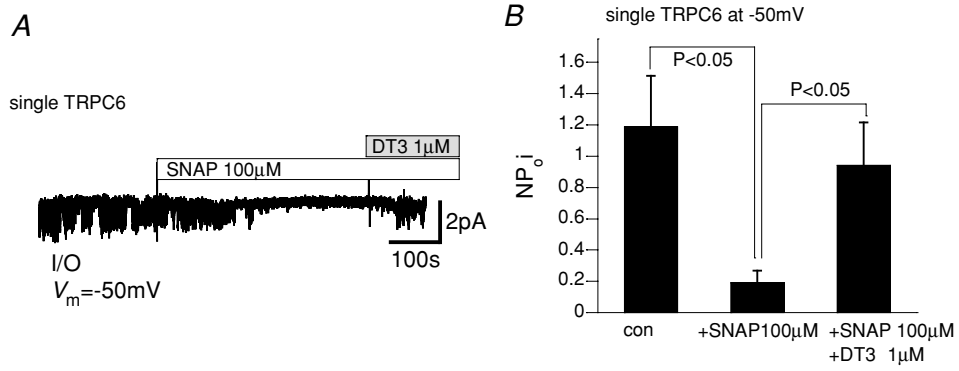

Figure 4. PKG-mediated inhibition of single TRPC6 channels
Inside-out (I/O) single channel recording. *A*, actual trace of single CCh (100 μM)-induced TRPC6 channel activities recorded at −50 mV. SNAP (100 μM) and DT3 (1 μM) were applied at the bars. Large vertical deflections reflect the artifacts of fast solution change via a 'Y-tube'. *B*, summary of the effects of SNAP and DT3 from 5 separate experiments. The mean single channel current (NP_oi) was calculated as the average of current amplitudes over 5 s.

AVP-induced membrane potential: -22.6 ± 1.4 mV, $n = 8$ *versus* -35.7 ± 4.8 mV, $n = 5$ for control and SNAP, respectively) with little influence on the resting membrane potential (-53.0 ± 2.4 mV, $n = 8$ *versus* -51.7 ± 2.3 mV, $n = 5$ for control and SNAP, respectively) (Fig. 8*E* and *F*). The seemingly weaker inhibitory effect of SNAP on AVP-induced depolarization than on the AVP-induced inward current may reflect the non-linearity of the

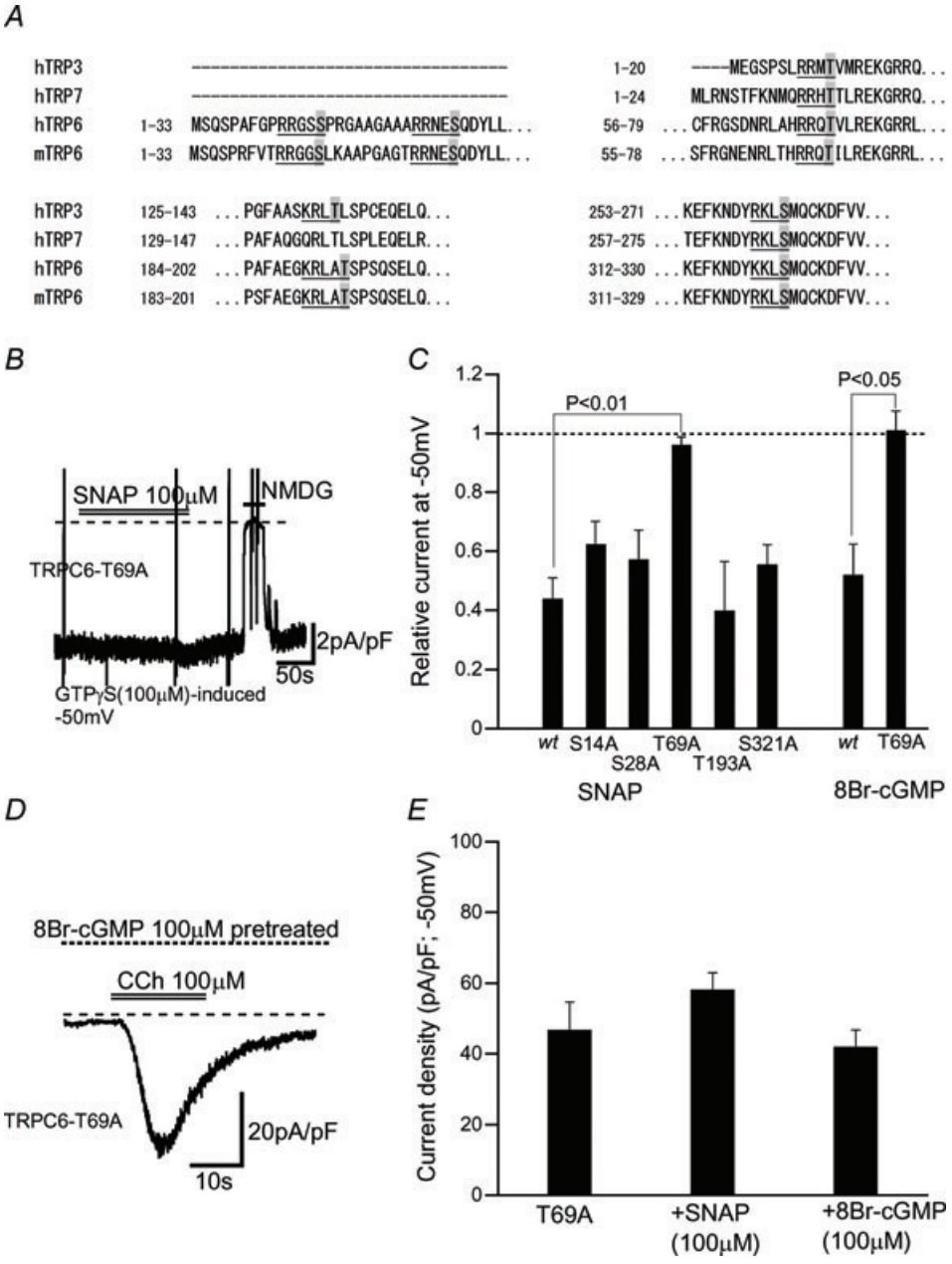

Figure 5. Influence of alanine substitutions for putative PKG phosphorylation sites on SNAP- or 8Br-cGMP-induced inhibition on I_{TRPC6}

A, Alignment by the program 'CLUSTALW of N-terminal amino acid sequences of murine TRPC6 (mTRPC6), human TRPC6 (hTRPC6), human TRPC3 (hTRPC3) and human TRPC7 (hTRPC7) channels. Five putative PKG phosphorylation motifs of mTRPC6 and those of other TRPC channels are underlined in which target serines or theronines are highlighted in grey. *B*, actual trace for GTPγS-induced I_{TRPC6} recorded from HEK cells expressing T69A TRPC6 mutant. Bath application of SNAP (100 μM) failed to inhibit the current, while Na^+ substitution with NMDG abolished it. *C*, summary for the inhibitory effects of SNAP (100 μM) or 8Br-cGMP (100 μM) on GTPγS-induced I_{TRPC6} in wild-type (wt) and five alanine-substitution mutant TRPC6-expressing HEK cells. $n = 5$–7. The definition of relative currents is the same as in Fig. 2. *D*, actual trace for CCh-induced I_{TRPC6} in a T69A-expressing HEK cell. *E*, summary of the inhibitory effects of SNAP (100 μM) and 8Br-cGMP (100 μM) on the density (−50 mV) of CCh-induced I_{TRPC6} at peak activation in T69A-expressing HEK cells. $n = 6$–7.

relationship between depolarization and conductance (Ginsborg, 1973).

In contrast, the closest homologue of TRPC6, TRPC7, which has been reported to be coexpressed in A7r5 myocytes and partially contributes to vasoconstrictor-induced cation currents (Maruyama *et al.* 2006), was rather quickly enhanced upon application of SNAP (Supplemental Fig. 3). This enhancement cannot account for the observed inhibition of cation current by SNAP in A7r5 cells. The inability of SNAP to inhibit TRPC7 channels may imply that a varying extent of heteromultimeric assembly between TRPC6 and TRPC7 proteins may generate the differential sensitivities of vasoconstrictor-activated cation channels to PKG regulation. We did not, however, further pursue this complicated aspect of TRPC6/TRPC7 heteromultimeric channel regulation by PKG in this study.

These results strongly suggest that PKG activation by NO–cGMP plays a pivotal role in the regulation of vasoconstrictor-induced cation entry and resulting depolarization which are closely associated with TRPC6 in A7r5 cells.

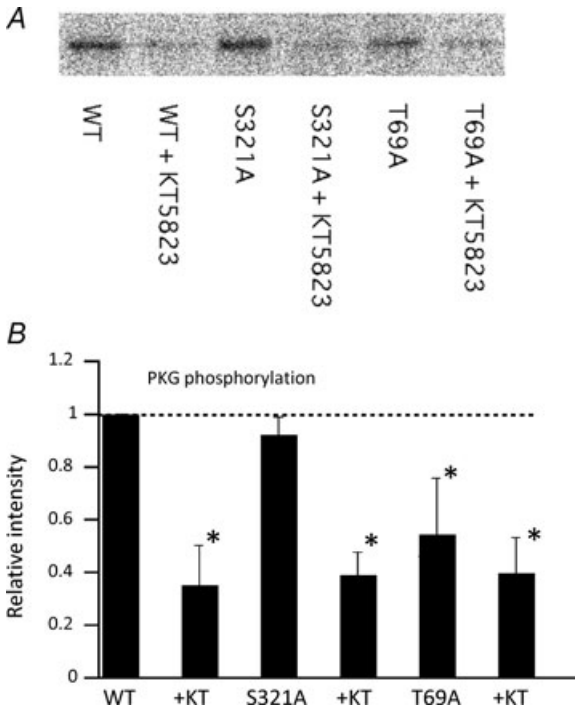

Figure 6. T69 is the site of phosphorylation by PKG
^{32}P-incorporation assay of wild-type and T69A- and S321A-mutant TRPC6 proteins. *A*, representative example of autoradiographed immunoblots by TRPC6-specific antibody after incubating TRPC6 proteins in ^{32}P-contating reaction solution with active PKGIα in the presence (+ KT) or absence of KT5823. In the T69A but not in the S321A mutant, the radioactivity of ^{32}P is significantly lowered. *B*, summary of ^{32}P-incorporation assay. ^{32}P-radioactivity is expressed as the fraction relative to that under control conditions (wild-type TRPC6 without KT5823) for each series of experiment. $n = 3$. $^*P < 0.05$.

Discussion

The results of the present study have provided the first functional evidence that TRPC6 channels are negatively regulated by PKG-mediated phosphorylation through the NO–cGMP signalling pathway. To explore this possibility, we conducted direct macroscopic and single channel current recordings with the patch clamp technique, and found that pharmacological blockade of the cGMP–PKG signalling with ODQ, KT5823 or DT3 PKG inhibitory peptide as well as site-directed alanine mutation of a PKG phosphorylation site (Thr69) abolished NO-induced inhibition of receptor-activated TRPC6 currents. Moreover, the critical involvement of Thr69 in PKG phosphorylation was also supported by the ^{32}P-incorporation assay of wild-type and alanine-substitution mutant TRPC6 proteins. Similar NO–cGMP–PKG-mediated negative regulation was also observed for TRPC6-like currents recorded from A7r5 VSMCs. Furthermore, membrane depolarization of A7r5 myocytes evoked by AVP, which is expected to secondarily activate VDCC, were significantly slowed and attenuated after application of the NO donor SNAP. TRPC6 protein is abundantly expressed in various types of VSMCs and has been shown to constitute vasoconstrictor-activated cation channels, which increase Ca^{2+} entry into VSMC via direct Ca^{2+} permeation or secondary activation of VDCC and/or Na^+–Ca^{2+} exchanger (Inoue *et al.* 2006; Dietrich *et al.* 2007; Poburko *et al.* 2007). Thus, it is highly plausible that, whether direct or indirect (i.e. via changes in membrane potential or increase in intracellular Na^+ concentration), PKG-mediated regulation may work as a universal negative feedback to neurohormonal Ca^{2+} mobilization across the VSMC membrane.

Emerging evidence suggests that NO regulates a wide range of target proteins via two distinct mechanisms, i.e. cGMP-dependent, PKG-mediated phosphorylation and GMP-independent S-nitrosylation. The latter mechanism manifests through direct covalent modification of reactive cysteine residues on target proteins, and is known to alter many ion channel activities. For instance, activation of the large-conductance Ca^{2+}-dependent K^+ channel (BK_{Ca}) is enhanced not only by PKG-mediated phosphorylation on Ser1072 of the $K_{Ca}1.1$ α-subunit C-terminus, which causes the hyperpolarizing shift of the Ca^{2+}-activation curve (Fukao *et al.* 1999), but also by *S*-nitrosylation under conditions devoid of cGMP (Bolotina *et al.* 1994; Lang & Watson, 1998). Similar but reciprocal regulation by NO has been demonstrated for the L-type VDCC whose voltage-dependent activation is inhibited by PKG-mediated phosphorylation but conversely enhanced by *S*-nitrosylation (Jian *et al.* 2007; Tjong *et al.* 2007). In contrast, for the canonical members of TRP channels, the two NO-mediated mechanisms appear to work separately. While members of the TRPC1/TRPC4/TRPC5 subfamily

are subject to direct activation by *S*-nitrosylation of cysteine residues (Cys553 and Cys558 in TRPC5) (Yoshida *et al.* 2006), those of the TRPC3/TRPC6/TRPC7 subfamily lacking the cysteines failed to be activated by NO *per se*, and instead were inhibited by the phosphorylation of threonine or serine residues by PKG (Kwan *et al.* 2004, 2006; this study). What is the physiological relevance of these two modes of NO-mediated regulation? One

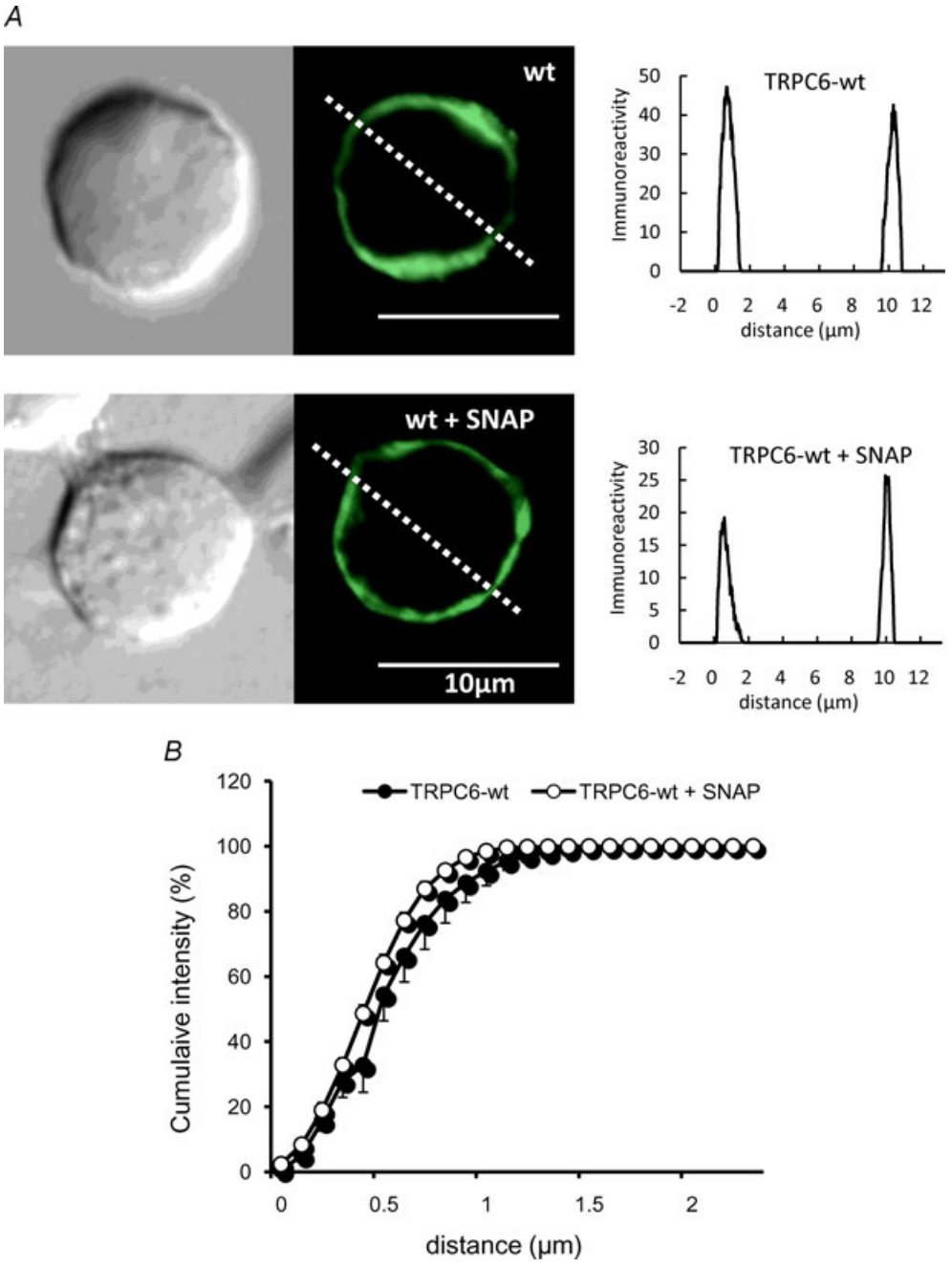

Figure 7. Immunolocalization of TRPC6 protein before and after SNAP treatment
A, representative of the immunofluorescence of TRPC6-expressing HEK293 cells before (upper) and after (lower) treatment with SNAP (100 μM) for 10 min. Left, phase-contrast image; middle, TRPC6 immunofluorescence; right, immunofluorescence intensity profile along the oblique dotted line in the middle panel. *B*, spatial distribution of TRPC6 immunofluorescence under SNAP-treated (○) and -untreated (●) conditions. Relative immunofluorescence of TRPC6 protein (expressed as percentage of total) integrated with respect to the distance from the surface to the cytosol of HEK cell is plotted as the function of distance (as indicated by dashed oblique lines in middle panels in *A*). Data represent the average from 5 to 6 cells.

possible hint may lie in the differential kinetics of the two reactions. In general, *S*-nitrosylation occurs through multiple chemical reactions without assistance of enzymes. Thus, it tends to need higher concentrations of NO and proceeds more slowly than cGMP–PKG-mediated actions (Ahern *et al.* 2002), as has been demonstrated for neuronal BK_{Ca} (Klyachko *et al.* 2001). This seems to match up with our present findings that inhibition of TRPC6

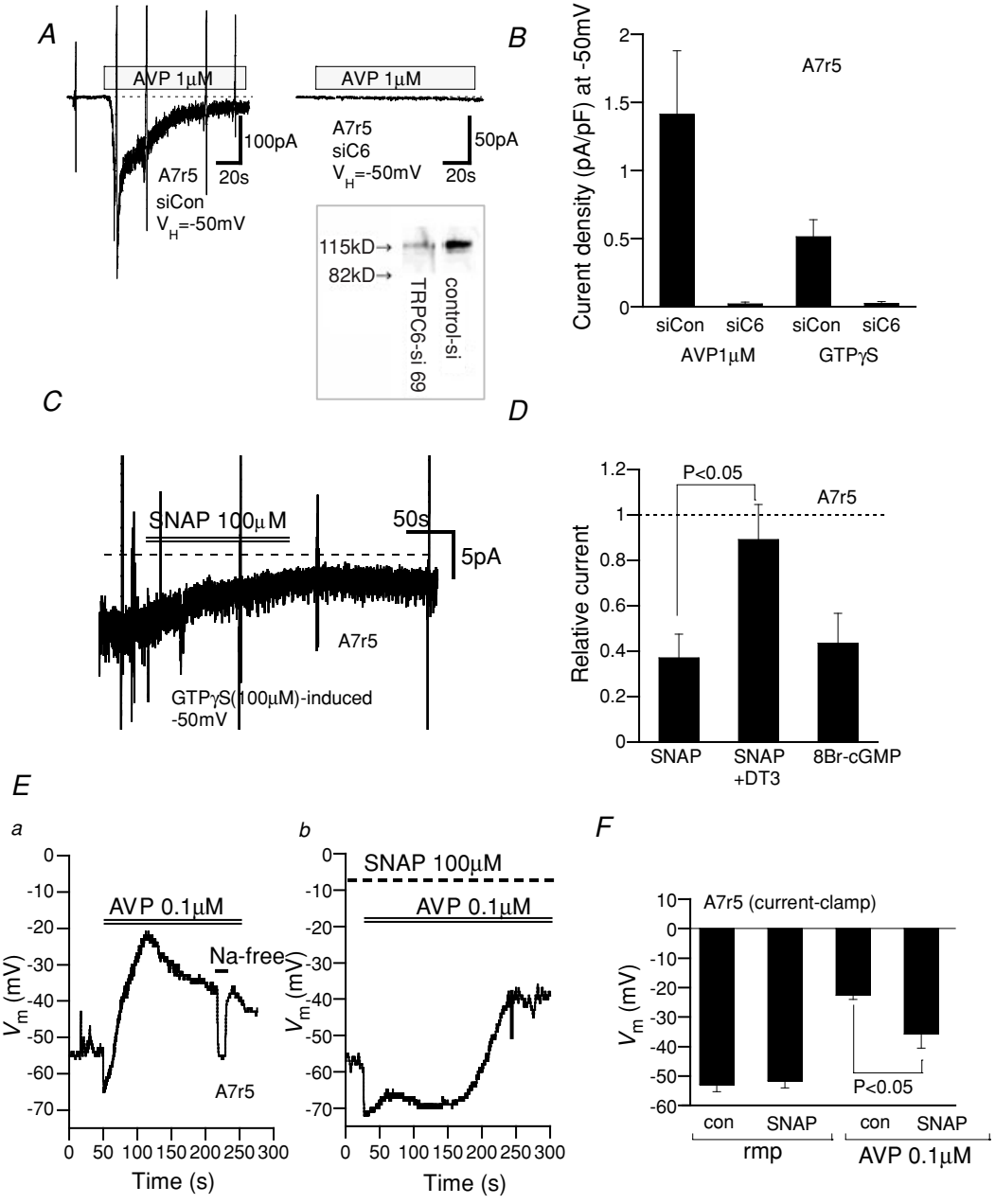

Figure 8. AVP-induced TRPC6-like cation currents and depolarization in A7r5 are negatively regulated by the cGMP–PKG pathway

Recording conditions are the same as in Figs 1 and 2. *A*, actual trace of AVP (1 μM)-induced cation current in A7r5 myocyte voltage-clamped at −50 mV without (left) and with (right) siRNA silencing of TRPC6. Inset, immunoblot of TRPC6 protein after 72 h siRNA knockdown. Control siRNA (siCon) and TRPC6-specific siRNA (siC6). *B*, current density (at −50 mV) of AVP- or GTPγS-induced cation currents without (left columns) and with (right columns) TRPC6-siRNA. $n = 5$. *C*, actual trace for SNAP inhibition of GTPγS-induced cation current in an A7r5 myocyte. *D*, relative current remaining after treatment with SNAP (100 μM) without and with inclusion of DT3 (1 μM) in the pipette or 8Br-cGMP (100 μM). $n = 4$–5. *E*, AVP (0.1 μM)-induced membrane depolarization in A7r5 myocytes under current clamp conditions in the absence (*a*) and presence (*b*) of SNAP (100 μM; 10 min pretreated). At the bars, AVP-containing or Na-free (equimolar substitution of Na^+ with NMDG) external solution were applied. *F*, summary of current clamp recordings as shown in *E*. $n = 5$–8.

current by SNAP (thus NO) occurred more rapidly (in tens of seconds; Fig. 2) and at lower concentrations (1–100 μM) compared with the reported kinetics of TRPC5 channel activation via *S*-nitrosylation (time to half-peak with 300 μM: ~5 min; 10 μM–1 mM) (Yoshida *et al.* 2006). These facts and the relative abundance of TRPC6 in VSMCs, may suggest that PKG-mediated phosphorylation may be more effective than *S*-nitrosylation under the physiological conditions. It is also conceivable that diffusion of NO between the sites of NO production (i.e. VECs and nitrergic nerve terminals) and PKG activation (VSMC) would tend to decrease the bioavailability of NO (Busse & Fleming, 2003; Toda & Okamura, 2003). This would then render *S*-nitrosylation less potent in VSMCs, while more predominant in VECs. Indeed, consistent with this idea, genetic deletion of PKG has been found to greatly impair the relaxant effects of the NO–cGMP pathway on pre-constricted blood vessels or contraction of VSMCs by vasoconstrictive agonists, suggesting the relative importance of a PKG-mediated inhibitory mechanism (Pfeifer *et al.* 1998). On the other hand, the expression of TRPC4 and TRPC5 may be more restricted to VECs, the site of NO production, and their activation by vasoactive agents (e.g. ACh, ATP) seems essential for NO production and its acceleration, where *S*-nitrosylation may play a vital role (Yoshida *et al.* 2006; Kwan *et al.* 2007). These facts collectively suggest that the sites for NO production and utilization are effectively separated by the differential expression of TRPC channels as well as their differential regulation by NO. It will thus be of great interest in future to examine how these two distinct mechanisms are coordinated *in situ* by, for example, live imaging techniques.

Mutagenesis scanning and phosphorylation assays have revealed that, amongst several possible PKG phosphorylation sites, only Thr69 (but not Ser321) on the N-terminus of TRPC6 channel, which is equivalent to one of the two PKG phosphorylation sites of TRPC3 channel Thr11 (Kwan *et al.* 2004), is critical for NO–cGMP-dependent TRPC6 channel regulation. Interestingly, another PKG phosphorylation site, Ser263 of TRPC3 (the TRPC6 equivalent is Ser321), has also been implicated in PKC-mediated phosphorylation that indirectly activates PKG and thereby inhibits the TRPC3 channel. However, we could not obtain evidence for this in TRPC6 channel regulation; alanine substitution of Ser321 failed to attenuate the NO–cGMP-mediated inhibition or phosphorylation of the TRPC6 channel (Fig. 6); the PKG inhibitor alone did not affect the receptor-activated TRPC6 currents (Fig. 3*E*). Thus, the two TRPC channels, albeit sharing a high degree of similarity in amino acid sequence, seem to undergo differential regulation via PKG and PKC, and this might help finely tune channel activity. Physiological implications of PKG-mediated regulation of the TRPC6 channel seem different from those of other phosphorylation-mediated regulations such as by PKC and CaMKII (Shi *et al.* 2004; Trebak *et al.* 2005; Yao *et al.* 2005). As shown previously, the contribution of the latter two kinases appears mostly restricted to the activation and inactivation time courses of the TRPC6 channel during or after PLC-linked receptor stimulation, respectively, as a consequence of a $[Ca^{2+}]_i$ rise and DAG generation. Consistent with this, the C-terminus of TRPC6 channel contains a competitive PIP_2–calmodulin binding region responsible for channel activation/inactivation processes in response to receptor stimulation (Kwon *et al.* 2007) and a critical serine residue (Ser768 in human) phosphorylated by PKC (Trebak *et al.* 2005). Interestingly, activation of this enzyme has reduced sensitivity to PIP_2-mediated TRPV1 channel inhibition (Szallasi *et al.* 2007). In contrast, NO–cGMP–PKG-mediated inhibition was persistent and did not change in its extent whether SNAP or 8Br-cGMP was applied before or after activation of the channel (Fig. 1*C* *versus* Figs 2*B* and 4). This indicates that phosphorylation of the TRPC6 channel by PKG causes inhibition regardless of receptor activation, and thus independent of PIP_2 hydrolysis induced by PLC activation. These notable differences may imply the presence of two mechanistically distinct modes of kinase-mediated regulation, i.e. the C-terminal, PIP_2–calmodulin-mediated and N-terminal, protein interaction-mediated regulation for the TRPC3/C6/C7 subfamily members. Similarly, two modes of regulation may be operative in VDCCs (Maier & Bers, 2002; Wu *et al.* 2002; Yang *et al.* 2007).

VSMCs are continuously exposed to NO liberated from neighbouring endothelial cells in response to blood flow and vasoactive substances and/or released from vascular nitrergic nerves. These physiological settings maintain VSMCs partially relaxed against vasoconstrictive drive via neurohormonal and myogenic mechanisms (Busse & Fleming, 2003; Toda & Okamura, 2003; Thorneloe & Nelson, 2005). Endothelial damage or dysfunction such as atherosclerosis impairs NO production and may bring VSMCs toward a more contractile status thereby predisposing to excessive vasoconstriction or vasospasm (Faxon *et al.* 2004). It has been shown that targeted deletion of the PKG Iα gene causes systemic hypertension accompanied by impaired NO–cGMP-dependent vasorelaxation of large and small arteries pre-constricted with noradrenaline (Pfeifer *et al.* 1998). This suggests the pivotal counteracting role of PKG-mediated phosphorylation against the hypertensive actions of neurohormonal effectors. In this respect, our present results have importantly demonstrated that, in addition to other mechanisms associated with VSMC $[Ca^{2+}]_i$ homeostasis, negative regulation of TRPC6 channels by PKG-mediated phosphorylation may serve as another vital mechanism lowering the blood pressure and maintaining local blood flow.

References

Ahern GP, Klyachko VA & Jackson MB (2002). cGMP and S-nitrosylation: two routes for modulation of neuronal excitability by. *Trends Neurosci* **25**, 510–517.

Bolotina VM, Najibi S, Palacino JJ, Pagano PJ & Cohen RA (1994). Nitric oxide directly activates calcium-dependent potassium channels in vascular smooth muscle. *Nature* **368**, 850–853.

Busse R & Fleming I (2003). Regulation of endothelium-derived vasoactive autacoid production by hemodynamic forces. *Trends Pharmacol Sci* **24**, 24–29.

Dietrich A, Kalwa H, Fuchs B, Grimminger F, Weissmann N & Gudermann T (2007). *In vivo* TRPC functions in the cardiopulmonary vasculature. *Cell Calcium* **42**, 233–244.

Faxon DP, Fuster V, Libby P, Beckman JA, Hiatt WR, Thompson RW, Topper JN, Annex BH, Rundback JH, Fabunmi RP, Robertson RM & Loscalzo J (2004). Atherosclerotic Vascular Disease Conference: Writing Group III: pathophysiology. *Circulation* **109**, 2617–2625.

Feil R, Lohmann SM, de Jonge H, Walter U & Hofmann F (2003). Cyclic GMP-dependent protein kinases and the cardiovascular system: insights from genetically modified mice. *Circ Res* **93**, 907–916.

Firth AL, Remillard CV & Yuan JX (2007). TRP channels in hypertension. *Biochim Biophys Acta* **1772**, 895–906.

Fukao M, Mason HS, Britton FC, Kenyon JL, Horowitz B & Keef KD (1999). Cyclic GMP-dependent protein kinase activates cloned BKCa channels expressed in mammalian cells by direct phosphorylation at serine 1072. *J Biol Chem* **274**, 10927–10935.

Ginsborg BL (1973). Electrical changes in the membrane in junctional transmission. *Biochem Biophys Acta* **300**, 289–317.

Hill AJ, Hinton JM, Cheng H, Gao Z, Bates DO, Hancox JC, Langton PD & James AF (2006). A TRPC-like non-selective cation current activated by α1-adrenoceptors in rat mesenteric artery smooth muscle cells. *Cell Calcium* **40**, 29–40.

Hisatsune C, Kuroda Y, Nakamura K, Inoue T, Nakamura T, Michikawa T, Mizutani A & Mikoshiba K (2004). Regulation of TRPC6 channel activity by tyrosine phosphorylation. *J Biol Chem* **279**, 18887–18894.

Hofmann F, Feil R, Kleppisch T & Schlossmann J (2006). Function of cGMP-dependent protein kinases as revealed by gene deletion. *Physiol Rev* **86**, 1–23.

Inoue R, Hai L & Honda A (2008). Pathophysiological implications of transient receptor potential channels in vascular function. *Curr Opin Nephrol Hypertens* **17**, 193–198.

Inoue R, Jensen LJ, Shi J, Morita H, Nishida M, Honda A & Ito Y (2006). Transient receptor potential channels in cardiovascular function and disease. *Circ Res* **99**, 119–131.

Inoue R, Okada T, Onoue H, Hara Y, Shimizu S, Naitoh S, Ito Y & Mori Y (2001). The transient receptor potential protein homologue TRP6 is the essential component of vascular a_1-adrenocepotor-activated Ca^{2+}-permeable cation channel. *Circ Res* **88**, 325–332.

Jian K, Chen M, Cao X, Zhu XH, Fung ML & Gao TM (2007). Nitric oxide modulation of voltage-gated calcium current by S-nitrosylation and cGMP pathway in cultured rat hippocampal neurons. *Biochem Biophys Res Commun* **359**, 481–485.

Karaki H, Ozaki H, Hori M, Mitsui-Saito M, Amano K, Harada K, Miyamoto S, Nakazawa H, Won KJ & Sato K (1997). Calcium movements, distribution, and functions in smooth muscle. *Pharmacol Rev* **49**, 157–230.

Klyachko VA, Ahern GP & Jackson MB (2001). cGMP-mediated facilitation in nerve terminals by enhancement of the spike afterhyperpolarization. *Neuron* **31**, 1015–1025.

Kuwahara K, Wang Y, McAnally J, Richardson JA, Bassel-Duby R, Hill JA & Olson EN (2006). TRPC6 fulfills a calcineurin signaling circuit during pathologic cardiac remodeling. *J Clin Invest* **116**, 3114–3126.

Kwan HY, Huang Y & Yao X (2004). Regulation of canonical transient receptor potential isoform 3 (TRPC3) channel by protein kinase G. *Proc Natl Acad Sci U S A* **101**, 2625–2630.

Kwan HY, Huang Y & Yao X (2006). Protein kinase C can inhibit TRPC3 channels indirectly via stimulating protein kinase G. *J Cell Physiol* **207**, 315–321.

Kwan HY, Huang Y & Yao X (2007). TRP channels in endothelial function and dysfunction. *Biochim Biophys Acta* **1772**, 907–914.

Kwon Y, Hofmann T & Montell C (2007). Integration of phosphoinositide- and calmodulin-mediated regulation of TRPC6. *Mol Cell* **25**, 491–503.

Lang RJ & Watson MJ (1998). Effects of nitric oxide donors, S-nitroso-L-cysteine and sodium nitroprusside, on the whole-cell and single channel currents in single myocytes of the guinea-pig proximal colon. *Br J Pharmacol* **123**, 505–517.

Lemonnier L, Trebak M & Putney JW Jr (2007). Complex regulation of the TRPC3, 6 and 7 channel subfamily by diacylglycerol and phosphatidylinositol-4,5-bisphosphate. *Cell Calcium* **43**, 506–514.

Lincoln TM, Dey N & Sellak H (2001). Invited review: cGMP-dependent protein kinase signaling mechanisms in smooth muscle: from the regulation of tone to gene expression. *J Appl Physiol* **91**, 1421–1430.

Lippincott-Schwartz J, Roberts TH & Hirschberg K (2000). Secretory protein trafficking and organelle dynamics in living cells. *Annu Rev Cell Dev Biol* **16**, 557–589.

Ma D & Jan LY (2002). ER transport signals and trafficking of potassium channels and receptors. *Curr Opin Neurobiol* **12**, 287–292.

McKinsey TA & Olson EN (2005). Toward transcriptional therapies for the failing heart: chemical screens to modulate genes. *J Clin Invest* **115**, 538–546.

Maier LS & Bers DM (2002). Calcium, calmodulin, and calcium-calmodulin kinase II: heartbeat to heartbeat and beyond. *J Mol Cell Cardiol* **34**, 919–939.

Maruyama Y, Nakanishi Y, Walsh EJ, Wilson DP, Welsh DG & Cole WC (2006). Heteromultimeric TRPC6-TRPC7 channels contribute to arginine vasopressin-induced cation current of A7r5 vascular smooth muscle cells. *Circ Res* **98**, 1520–1527.

Pfeifer A, Klatt P, Massberg S, Ny L, Sausbier M, Hirneiss C, Wang GX, Korth M, Aszodi A, Andersson KE, Krombach F, Mayerhofer A, Ruth P, Fassler R & Hofmann F (1998). Defective smooth muscle regulation in cGMP kinase I-deficient mice. *EMBO J* **17**, 3045–3051.

Poburko D, Liao CH, Lemos VS, Lin E, Maruyama Y, Cole WC & van Breemen C (2007). Transient receptor potential channel 6-mediated, localized cytosolic [Na^+] transients drive Na^+/Ca^{2+} exchanger-mediated Ca^{2+} entry in purinergically stimulated aorta smooth muscle cells. *Circ Res* **101**, 1030–1038.

Ramsey IS, Delling M & Clapham DE (2006). An introduction to TRP channels. *Annu Rev Physiol* **68**, 619–647.

Saleh SN, Albert AP, Peppiatt CM & Large WA (2006). Angiotensin II activates two cation conductances with distinct TRPC1 and TRPC6 channel properties in rabbit mesenteric artery myocytes. *J Physiol* **577**, 479–495.

Shi J, Mori E, Mori Y, Mori M, Li J, Ito Y & Inoue R (2004). Multiple regulation by calcium of murine homologues of transient receptor potential proteins TRPC6 and TRPC7 expressed in HEK293 cells. *J Physiol* **561**, 415–432.

Shi J, Takahashi S, Jin XH, Li YQ, Ito Y, Mori Y & Inoue R (2007). Myosin light chain kinase-independent inhibition by ML-9 of murine TRPC6 channels expressed in HEK293 cells. *Br J Pharmacol* **152**, 122–131.

Soboloff J, Spassova M, Xu W, He LP, Cuesta N & Gill DL (2005). Role of endogenous TRPC6 channels in Ca^{2+} signal generation in A7r5 smooth muscle cells. *J Biol Chem* **280**, 39786–39794.

Szallasi A, Cortright DN, Blum CA & Eid SR (2007). The vanilloid receptor TRPV1: 10 years from channel cloning to antagonist proof-of-concept. *Nat Rev Drug Discov* **6**, 357–372.

Takahashi S, Kawarabayashi Y, Hai L, Honda A & Inoue R (2007). Protein kinase G (PKG)-mediated tonic inhibition of vascular transient receptor potential (TRP) channel TRPC6. *J Physiol Sci* **57**, S78.

Thorneloe KS & Nelson MT (2005). Ion channels in smooth muscle: regulators of intracellular calcium and contractility. *Can J Physiol Pharmacol* **83**, 215–242.

Tjong YW, Jian K, Li M, Chen M, Gao TM & Fung ML (2007). Elevated endogenous nitric oxide increases Ca^{2+} flux via L-type Ca^{2+} channels by S-nitrosylation in rat hippocampal neurons during severe hypoxia and in vitro ischemia. *Free Radic Biol Med* **42**, 52–63.

Toda N & Okamura T (2003). The pharmacology of nitric oxide in the peripheral nervous system of blood vessels. *Pharmacol Rev* **55**, 271–324.

Trebak M, Hempel N, Wedel BJ, Smyth JT, Bird GS & Putney JW Jr (2005). Negative regulation of TRPC3 channels by protein kinase C-mediated phosphorylation of serine 712. *Mol Pharmacol* **67**, 558–563.

Vazquez G, Wedel BJ, Kawasaki BT, Bird GS & Putney JW Jr (2004). Obligatory role of Src kinase in the signaling mechanism for TRPC3 cation channels. *J Biol Chem* **279**, 40521–40528.

Wu L, Bauer CS, Zhen XG, Xie C & Yang J (2002). Dual regulation of voltage-gated calcium channels by PtdIns(4,5)P_2. *Nature* **419**, 947–952.

Yang L, Liu G, Zakharov SI, Bellinger AM, Mongillo M & Marx SO (2007). Protein kinase G phosphorylates Cav1.2 α1c and β2 subunits. *Circ Res* **101**, 465–474.

Yao X, Kwan HY & Huang Y (2005). Regulation of TRP channels by phosphorylation. *Neurosignals* **14**, 273–280.

Yoshida T, Inoue R, Morii T, Takahashi N, Yamamoto S, Hara Y, Tominaga M, Shimizu S, Sato Y & Mori Y (2006). Nitric oxide activates TRP channels by cysteine S-nitrosylation. *Nat Chem Biol* **2**, 596–607.

Acknowledgements

We are grateful to Professor Alison Brading at the Department of Pharmacology, University of Oxford, for English correction. We also thank Prof. Kihachiro Abe, at Special Oral Care Unit, Kyushu University Hospital, for giving a chance to conduct the present work to S.T. This work was supported in part by a grant-in-aid from the Japan Society of the Promotion of Science (No. 17590221).

Supplemental material

Online supplemental material for this paper can be accessed at: http://jp.physoc.org/cgi/content/full/jphysiol.2008.156083/DC1